

The Marine Algal Virus PpV01 Has an Icosahedral Capsid with T=219 Quasisymmetry

Xiaodong Yan,¹† Paul R. Chipman,¹ Tonje Castberg,² Gunnar Bratbak,²
and Timothy S. Baker^{1*}

Department of Biological Sciences, Purdue University, West Lafayette, Indiana 47907,¹ and Department of Microbiology, University of Bergen, N-5020 Bergen, Norway²

Received 3 February 2005/Accepted 13 March 2005

***Phaeocystis pouchetii* virus (PpV01) infects and lyses the haptophyte *Phaeocystis pouchetii* (Hariot) Lagerheim and was first isolated from Norwegian coastal waters. We have used electron cryomicroscopy and three-dimensional image reconstruction methods to examine the native morphology of PpV01 at a resolution of 3 nm. The icosahedral capsid of PpV01 has a maximum diameter of 220 nm and is composed of 2,192 capsomers arranged with T=219 quasisymmetry. One specific capsomer in each asymmetric unit contains a fiber-like protrusion. Density attributed to the presence of a lipid membrane appears just below (inside) the capsid. PpV01 is the largest icosahedral virus whose capsid structure has been determined in three dimensions from images of vitrified samples. Striking similarities in the structures of PpV01 and a number of other large double-stranded DNA viruses are consistent with a growing body of evidence that they share a common evolutionary origin.**

Phaeocystis pouchetii virus (PpV01) infects and lyses the haptophyte *Phaeocystis pouchetii* (Hariot) Lagerheim and was first isolated from Norwegian coastal waters in 1995 (17). The phytoplankton host of PpV01 is a representative of a genus with worldwide distribution and plays an important role in marine primary production and in ocean climate control. *Phaeocystis* spp. form dense, almost monospecific, blooms in polar waters and coastal regions, where they can be responsible for a large percentage of the total annual biomass production (11, 22). Cell lysis is a major factor in the declination of *Phaeocystis* blooms in the North Sea (7) and is possibly caused by viral infection (17). The genus *Phaeocystis* is a well-known producer of beta-dimethylsulfoniopropionate, which, through various processes including virus infection, leads to elevated levels of the biogenic trace gas dimethyl sulfide (DMS), the second most important source of atmospheric sulfur. Because DMS is known to promote cloud formation when emitted to the atmosphere, sea-to-air emission of DMS is a key pathway in the global sulfur cycle (4, 24). Infection of *P. pouchetii* by PpV01 may thus have a direct impact on ocean climate. In addition, during cell lysis, proteins and other polymers are released that may contribute to the formation of foam. *Phaeocystis* is notoriously known for foam formation along the European continental coast (21).

Relatively little is known about the biochemistry of PpV01, and even less is known about its structure. Preliminary characterization by negative-stain, transmission electron microscopy has shown free viral particles to be spherical, ranging in diameter from 130 to 170 nm, and devoid of appendages or a

tail (17). In thin sections, PpV01 is 130 to 160 nm in diameter and often exhibits hexagonal profiles, suggesting that virions may contain an icosahedrally symmetric capsid. Viral assembly occurs in the cytoplasm of infected cells, and as viral production progresses, organelles are disrupted and the cell wall lyses (17). The viral genome consists of a 485-kbp double-stranded DNA (dsDNA) (9) whose sequence has yet to be determined. PpV01 virions primarily contain an ~59-kDa protein and at least five minor proteins ranging in mass from 30 to 50 kDa (17). To date, there are no known reports concerning the stoichiometries of these components or of the possible lipid composition of PpV01. Though PpV01 has yet to be assigned taxonomically, it shares a number of common properties with members of the *Phycodnaviridae*.

In this study, we have used cryoelectron microscopy (cryo-EM) and three-dimensional (3-D) image reconstruction methods to examine the native morphology of PpV01 at a resolution of 3 nm. PpV01 possesses an icosahedral capsid (largest dimension is 220 nm) comprised of 2,192 capsomers arranged with T=219 quasisymmetry; 60 fiber-like protrusions decorate the outer surface of the capsid; and characteristic features we attribute to a lipid membrane lie beneath the capsid. To date, PpV01 has the largest triangulation symmetry among all the icosahedral viruses studied and has the largest diameter among all viruses whose capsid structure has been determined in three dimensions from images of vitrified samples. Similarity of the PpV01 capsid structure to a number of other large dsDNA viruses strongly supports other lines of evidence that point to close evolutionary ties among these viruses (6, 16, 31).

MATERIALS AND METHODS

Isolation and purification of PpV01. Samples of PpV01 for cryo-EM studies were isolated and purified as described previously (17). *Phaeocystis pouchetii* strain AJ01 was cultured in f/2 medium (15) at 5°C under a 14:10 h light:dark cycle using white light from fluorescent tubes at a level of about 30 $\mu\text{mol photons m}^{-2} \text{ s}^{-1}$. Cultures were infected with PpV01 in the late exponential growth phase. After 96 h, the cultures were completely lysed and cell debris was removed

* Corresponding author. Present address: Department of Chemistry & Biochemistry and Molecular Biology, University of California, San Diego, La Jolla, CA 92093-0378. Phone: (858) 534-5845. Fax: (858) 534-5846. E-mail: tsb@chem.ucsd.edu.

† Present address: Department of Chemistry & Biochemistry and Molecular Biology, University of California, San Diego, La Jolla, CA 92093-0378.

by low-speed centrifugation ($10,000 \times g$, 20 min). Viruses were then pelleted by ultracentrifugation ($100,000 \times g$, 60 min). The pellets were resuspended in Tris-buffered saline, and viruses were purified by sucrose gradient (10 to 40%) centrifugation ($50,000 \times g$, 30 min). The virus band, extracted with a syringe, was diluted in Tris-buffered saline, and the viruses were then pelleted by ultracentrifugation to remove sucrose. This virus pellet was resuspended in Tris-buffered saline with 0.01% sodium azide for use in cryo-EM experiments.

cryo-EM and 3-D image reconstruction of PpV01. Purified PpV01 samples at a concentration of ~ 1 mg/ml were vitrified for cryo-EM as described previously (3). Images were recorded on Kodak SO-163 film at $\times 33,000$ nominal magnification in a Philips CM300 FEG microscope at 300 kV, at underfocus settings estimated to be between $1.0 \mu\text{m}$ to $2.0 \mu\text{m}$, and with an electron dose of $2,200 \text{ e}^-/\text{nm}^2$. Visual inspection of the 87 recorded micrographs led to 46 being selected for digitization with a step size of $7 \mu\text{m}$ on a Zeiss Phodis microdensitometer. These scanned data were then bin averaged to yield pixels with an effective size at the sample of 0.636 nm . A total of 982 PpV01 particle images were extracted from these micrographs using the manual boxing protocol included in the RobEM interactive graphics program (http://bilbo.bio.purdue.edu/~workshop/help_robem/). The origin and orientation parameters for each of these particle images were estimated by means of model-based procedures (2), and an electron density map of the T=169d *Paramecium bursaria Chlorella* virus 1 (PBCV-1) (35) served as the initial search model. Iterative refinement of the particle parameters was carried out in several cycles, and a final 3-D density map was computed to a resolution limit of 3.0 nm from 560 particles images as described previously (2, 36). The effective resolution of the density map was determined to be 3.0 nm . This was assessed by randomly sorting the particle images into two sets from which independent reconstructions were computed, and standard Fourier shell correlation (0.5) and phase difference criteria (45 degrees) were utilized (3, 36). The reconstructed map is arbitrarily displayed as the right (dextro) enantiomer, though the actual handedness needs to be determined (for an example, see reference 5).

In this study, no attempts were made to compensate for the effects of the microscope contrast transfer function (CTF). This in part reflects the difficulty in accurately determining the defocus level in thick samples and also in samples in which only a few particles typically appear in the field of view of each micrograph. The large diameter of PpV01 also produces a correspondingly large defocus gradient across each particle in the direction of the imaging beam and, hence, necessitates more elaborate and extensive processing schemes to compensate for the restricted depth of field (12, 18), even at moderate resolutions. In this study, where the resolution is limited to 3.0 nm , no data beyond the first node of the CTF for any micrograph was included in the 3-D reconstruction, and therefore, CTF-induced artifacts are reduced. Note that, for defocus settings in the 1.0 - to 2.0 - μm range, the first CTF node would occur between 1.4 and 2.0 nm resolution, respectively, which is well beyond the 3.0 nm cutoff of the present analysis.

RESULTS

cryo-EM of PpV01. When PpV01 is examined by conventional negative-stain techniques, it appears to be deformed or disrupted easily and it is difficult to detect any regular structure (data not shown). However, when PpV01 is embedded in vitreous ice, particles exhibit a variety of characteristic profiles, including both hexagonal and circular outlines consistent with icosahedral particle morphology (Fig. 1). The samples we examined consisted predominantly of empty particles (devoid of DNA genome) exhibiting a maximum diameter of $\sim 220 \text{ nm}$. In addition, most vitrified PpV01 particles contain what appears to be an asymmetric, liposome-like vesicle in contact with the inner surface of the capsid shell (Fig. 1). These observations contrast with our cryo-EM studies of three other large dsDNA viruses, PBCV-1 (35), chilo iridescent virus (CIV) (35), and frog virus 3 (FV3) (34), all of which contain significantly higher densities within their central cores. Indeed, thin-sectioned PpV01 also displays high-density core material consistent with the presence of the large genome (17). Though virions may have lost their genomes and some of the bilayer membrane during preparation procedures, nonetheless, our ability to reconstruct the 3-D structure of the PpV01 capsid to ~ 3 -nm

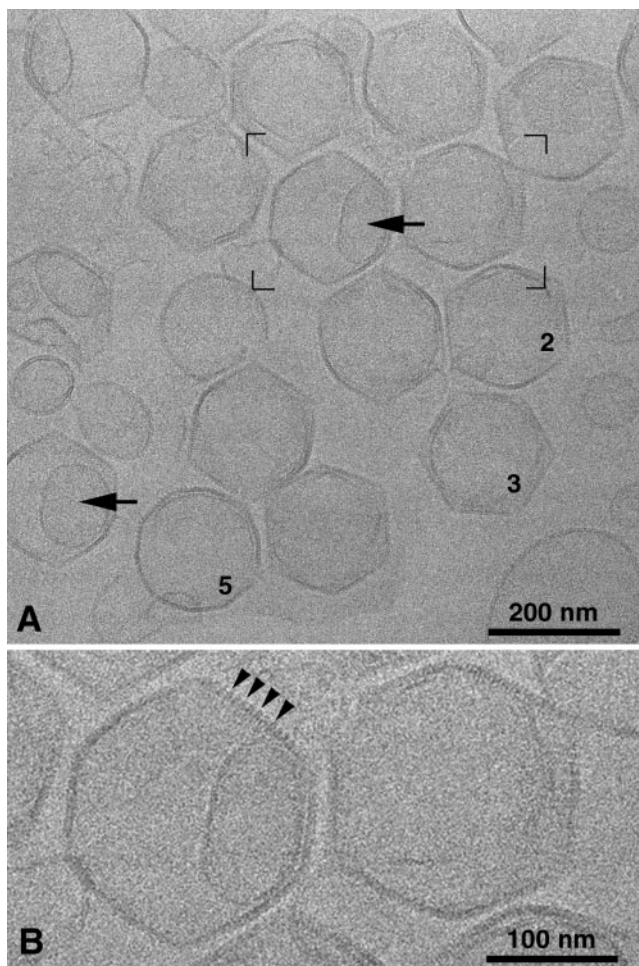


FIG. 1. Micrograph of vitrified sample of PpV01 empty capsids. (A) PpV01 exhibits a well-defined outer capsid and some particles contain vesicle-like inclusions (arrows). Representative particles oriented with their 2-, 3-, or 5-fold axes nearly parallel to the view direction are identified with numbers. (B) An enlarged view of the outlined area from panel A shows a highly serrated profile (arrowheads) in an edge of one capsid shell. Such a serrated appearance is characteristic of the presence of aligned arrays of distinct morphological units (capsomers).

resolution is compelling evidence that the capsid structure is rigid and complete. Unlike PpV01, in our analysis of FV3 (34), we found that most of the FV3 particles in vitrified samples were disrupted at one or more vertices with fivefold symmetry (5-fold vertices), and this led to a 3-D reconstruction in which the capsid density was much weaker near the 5-fold vertices than all other regions. In the present study of PpV01, the 3-D reconstruction map exhibits equally strong density in all regions of the capsid shell, which is consistent with the PpV01 capsid having a relatively stable and unique as well as complete structure.

The PpV01 capsid is organized with T=219 quasisymmetry. The 3-D image reconstruction of PpV01 reveals a number of morphological features (Fig. 2). The capsid has a distinct icosahedral shape, with a maximum outer diameter of 220 nm between opposed vertices. The diameter drops to 190 nm along the icosahedral 2- and 3-fold directions. The size of PpV01 is

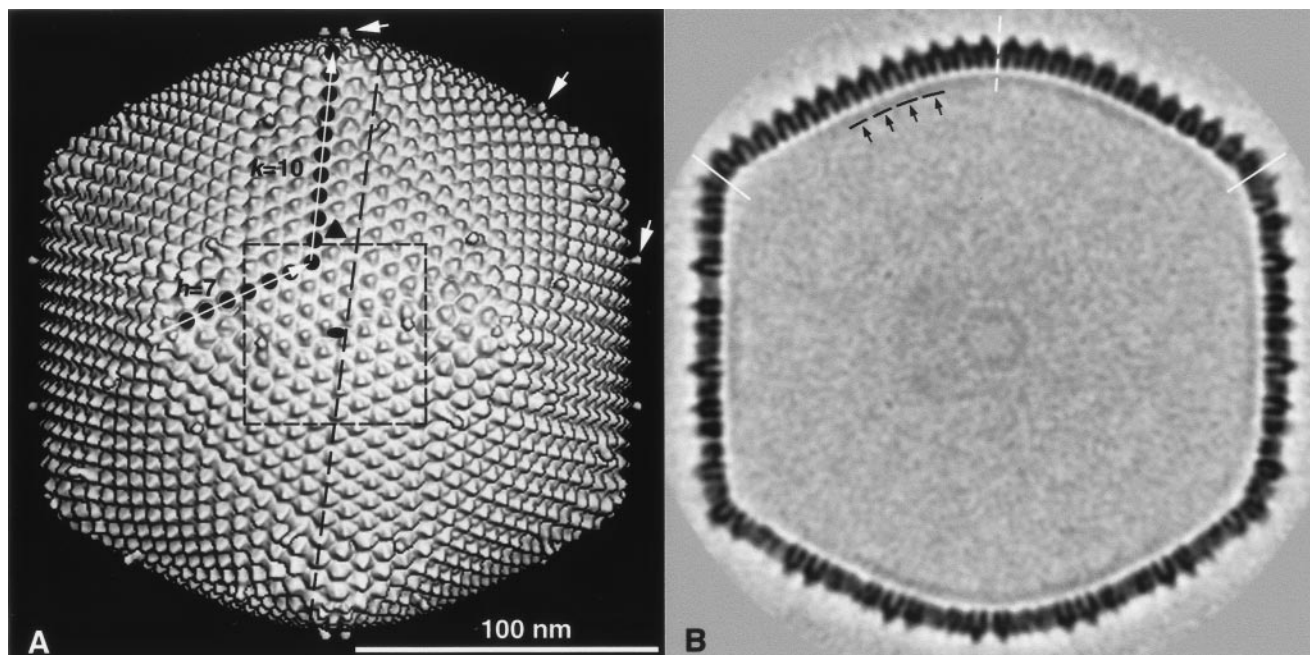


FIG. 2. PpV01 reconstruction. (A) Shaded-surface representation of the PpV01 3-D reconstruction, viewed along a 2-fold axis (ellipse); (B) nonequatorial density section (~ 0.6 nm thick; darkest features represent highest density) extracted in an orientation given by the dashed line in panel A. The locations of one icosahedral 2-fold (ellipse) and one 3-fold (triangle) axis of symmetry are marked with symbols. The T=219 dextrolattice ($h = 7, k = 10$) is specified by the pathway (black dots) of hexavalent capsomers between adjacent 5-fold vertices. For a T=219 lattice, the pathway is defined by 7 steps in the h direction followed by 10 steps in the k direction. The region bound by the dashed square is enlarged in Fig. 3A. The dashed line identifies the orientation of the cross-section view in panel B and follows a continuous line of 25 capsomers (between the solid white lines at the top of panel B), all of which are cross-sectioned at or near their centers. In panel B, black arrows and the black dashed line draw attention to the lipid bilayer, which appears as a faint and diffuse band of density that lies just below the inner wall of the capsid. The dashed white line lies close to an icosahedral 2-fold axis.

quite dramatic relative to, for example, the P=3 (pseudo T=3) human rhinovirus (37), which is more than seven times smaller in diameter and, hence, occupies 390 times less volume. Unlike rhinovirus, whose capsid consists of 180 subunits, thousands of knob-like capsomers are regularly arranged and form the capsid shell of PpV01. Close inspection of the PpV01 reconstruction shows a capsid consisting of 2,192 capsomers arranged in a T=219 icosahedral lattice ($h = 7, k = 10$) (8). In a T=219 lattice, there are 12 pentavalent and 2,180 hexavalent capsomers (27), with one hexavalent capsomer sitting exactly on each icosahedral 3-fold axis (Fig. 2A), as also occurs for the T=147 CIV (35). However, no capsomer occupies a 3-fold axis position in the T=169d PBCV-1 (35). In addition to the prominent array of capsomers, 60 fiber-like structures project radially above the PpV01 capsid and are nearly uniformly distributed over the surface (Fig. 2A).

When viewed in cross-section (Fig. 2B), the PpV01 density map reveals a highly ordered capsid shell that surrounds a nearly empty interior. Just beneath the ~ 6 -nm-thick shell lies a faint band of density that we attribute to a lipid membrane, owing to its similar location and appearance to the bilayer membranes observed in PBCV-1 and CIV (35). In PpV01 empty capsids, however, this membrane appears much less distinct because it is not confined by the presence of the genome and other core components and, hence, may not be uniform or highly organized. Though the presence of lipids in PpV01 has yet to be demonstrated biochemically, the unpro-

essed images and the reconstructed density map strongly support the presence of a bilayer, just as has been observed in other large icosahedral dsDNA viruses, like PBCV-1 (35), CIV (35), and FV3 (34).

As can be seen in surface views (Fig. 2A), in certain directions, as many as 25 capsomers are aligned in a continuous arc (Fig. 2A) that traverses two faces of the icosahedron. One such line of capsomers can be seen in cross-section (Fig. 2B, top), with 13 of them (Fig. 2B) nearly perfectly bisected and the other 12 viewed with the section plane slightly away from their centers. The remaining capsomers in the density section (Fig. 2B) are cut in a variety of positions because they lie various distances above or below as well as in the plane of the section.

The hexavalent capsomers are trimeric structures. Close inspection of the PpV01 reconstruction shows that all but one of the hexavalent capsomers in each asymmetric unit of the icosahedron have similar morphologies (Fig. 3). Shaded-surface (Fig. 3A) and sectioned (Fig. 3A, inset, and B) views show these capsomers to be hollow cylinders at their bases (~ 7 -nm diameter) and capped by a knob-like feature (cap) at the top. Each capsomer is ~ 9 nm high and includes ~ 6 nm for the cylinder portion and ~ 3 nm for the cap. Horizontal cross-sections at various heights along the cylinder axis (Fig. 3B) illustrate how the structure transforms from a hexameric shape at the base (closest to the center of the virion) to one that is trimeric at higher radii. Except for the presence of the cap, the morphology of each of the hexavalent capsomers in PpV01 is

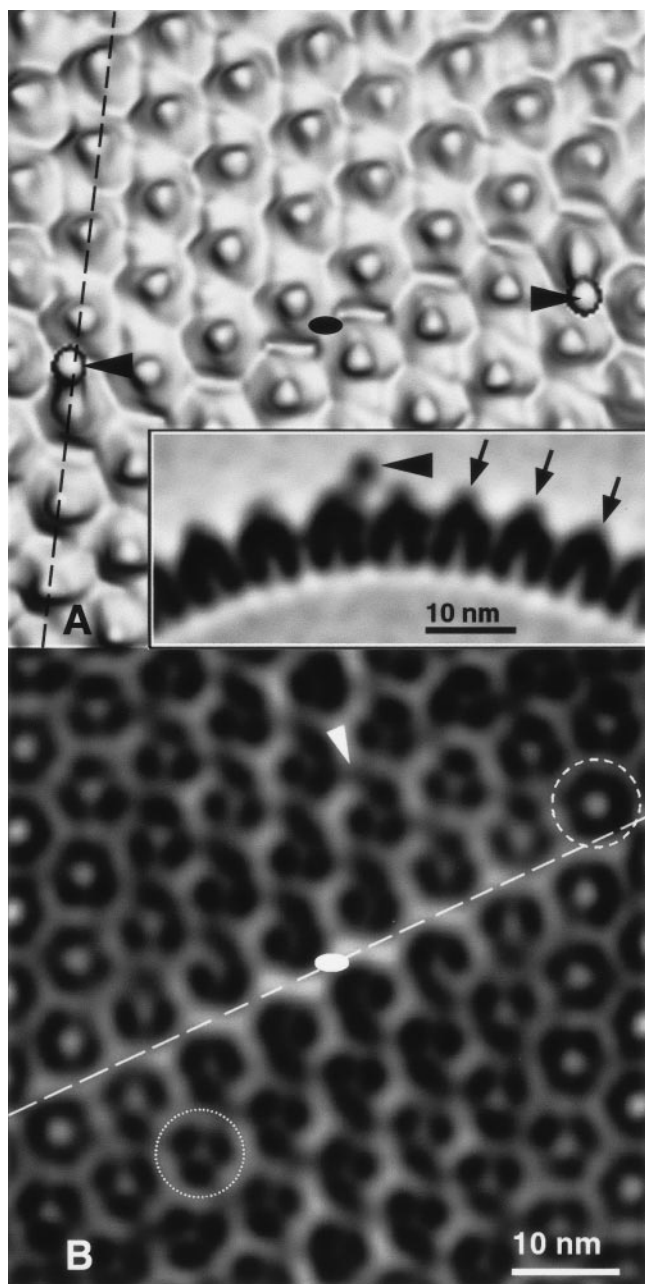


FIG. 3. Enlarged views of the PpV01 reconstruction, rendered as a shaded surface (A) and as a planar density section (~ 0.6 nm thick) (B). In panels A and B, the view direction is along a 2-fold axis (black and white ellipses). The inset in panel A is a cross-section perpendicular to the surface and in the direction indicated by the dashed line in panel A. Capsomers exhibit a pyramid-like morphology at the surface with a base of diameter ~ 7 nm. Beneath the surface (inset), each capsomer exhibits a hollow cylindrical shape, with a height of ~ 6 nm and a base of inner and outer diameters of ~ 2.1 and ~ 7 nm, respectively. Two capsomers in the field of view clearly differ from the others in that they contain fiber-like structures (black arrowheads in panel A and inset) that protrude at a 45° angle away from the capsomer axis. In panel B, where the plane of the section intersects at different levels along the axes of different capsomers, some capsomers appear trimeric (dotted circle), whereas others appear hexameric (dashed circle), consistent with each capsomer being comprised of a hexameric base and a trimeric top. Within the field of view (B), capsomers are organized into two oppositely oriented, quasihexagonal arrays, one above and the other below the dashed white line. In each array, the capsomers are close

quite similar to that of the hexavalent capsomers of PBCV-1 and CIV, which are trimers of the respective major capsid proteins (25, 35). The atomic structure of the PBCV-1 trimer clearly revealed how a hexameric base and a trimeric top arise from the quaternary arrangement of the large and small domains of the PBCV-1 Vp54 protein (25). In addition, Vp54 forms a “double-barrel trimer” structure that closely matches the pseudo-hexagonal cores of both the adenovirus hexon (28) and the bacteriophage PRD-1 P3 coat protein (1). Homology modeling of the major capsid proteins of several other dsDNA viruses, including those from CIV, Bam35, African swine fever virus, and mimivirus, also strongly suggests that they form double-barrel trimers (6). Hence, the hexavalent capsomers of PpV01 are likely to represent yet another example of this viral building block motif.

All 2,180 hexavalent capsomers in PpV01 have the same doughnut-like cylinder structure with hexameric and trimeric regions. Based on structural similarities as well as the sizes of the PBCV-1 and CIV major capsid proteins (54 and 48 kDa, respectively), the PpV01 hexavalent capsomers are most likely trimers of the 59-kDa PpV01 major capsid protein. Hence, assuming the pentavalent capsomers are comprised of a different viral protein, the T=219 PpV01 capsid must contain 6,540 copies ($= 3 \times 2,180$) of the major capsid protein. This differs from the 13,140 that would occur if the structure consisted of hexamers and pentamers, as first envisioned by Caspar and Klug (8) for small, spherical virus capsids. It is not possible at 3-nm resolution to determine whether the major capsid protein of PpV01 accounts solely for the density in the cylinder or if it is also included in the cap.

The PpV01 capsid contains 60 fibers. The one hexavalent capsomer that differs from all others in each of the 60 asymmetric units of the icosahedron does so because an asymmetric, protruding density feature (fiber) extends ~ 6 nm above the cap at an angle of $\sim 45^\circ$ with respect to the radial direction (Fig. 3A and inset). The small number and distribution of these fibers and their small size relative to the entire PpV01 virion renders them essentially invisible in unprocessed micrographs (Fig. 1). Nonetheless, the density of these asymmetric fibers is nearly as strong as that of the capsomers, indicating that the fibers are icosahedrally organized and have a rigid and well-defined asymmetric structure.

Though the identity and composition of the fibers have yet to be characterized, we presume that the fibers represent 60 copies of one or more minor structural proteins, and each fiber only binds to the unique hexavalent capsomer in each asymmetric unit. At 3-nm resolution, the reconstruction does not provide any obvious clues regarding how only these capsomers bind fibers. PBCV-1 has 60 bean-like protrusions that are also evenly distributed on its surface (data not shown). In contrast, CIV has 1,460 fibers that contain both rigid (proximal part) and flexible (distal part) domains (40 nm long and 1.5 nm in diameter) (35). It has been proposed that these viral protrusions

packed and all have the same or quite similar orientations. The interface between these two arrays appears as a less-dense region because the capsomers in the opposing arrays are not as tightly packed as in each individual array, where many thin, bridging density features (white arrowhead) appear to interconnect neighboring capsomers.

sions, which extend well above the capsid surface, may contain receptor recognition sites that enable virions to recognize and bind to their hosts (32). Fibers in PpV01 may serve a similar function.

The PpV01 capsid contains 20 trisymmetrons and 12 pentasymmetrons. Wrigley's pioneering electron microscopy study of *Sericesthis* iridescent virus demonstrated the existence of large, well-ordered capsid substructures (33). These groups of capsomers, termed trisymmetrons and pentasymmetrons, centered on the icosahedral 3-fold and 5-fold axes, respectively, were postulated to be subassembly units that might form characteristic building blocks in many if not all icosahedral capsids in very large viruses (33). Indeed, just as was found in PBCV-1 and CIV (35), the PpV01 capsid consists of 20 trisymmetrons and 12 pentasymmetrons (Fig. 4). In each of these viruses, the pentasymmetron contains 31 capsomers (1 pentamer plus 30 trimers). However, the different number of capsomers in each trisymmetron is one clear distinction among these viruses. The trisymmetron in PpV01 is an equilateral triangle with 13 trimers along an edge (~100 nm in length) and 91 trimers in all. In PBCV-1 and CIV, the trisymmetron consists of 66 (11 per ~90-nm edge) and 55 (10 per ~80-nm edge) trimers, respectively.

DISCUSSION

PpV01 has the largest diameter and T number of any icosahedral virus studied by cryo-EM reconstruction at 3-nm resolution or better. Just how a capsid consisting of 2,180 trimeric capsomers and 12 pentameric capsomers is able to assemble into such a precise, icosahedral structure remains an intriguing mystery.

Wrigley's study (33) of the capsid structure of *Sericesthis* iridescent virus (SIV), in which he observed and characterized both triangular and pentagonal facets, led him to propose the names "trisymmetron" and "pentasymmetron" for these facets. He further hypothesized that these facets represented key assembly intermediates for SIV as well as other large, icosahedral viruses. Whether tri- and pentasymmetrons do represent naturally occurring assembly intermediates for many if not all large, icosahedral virus capsids, remains to be determined. Nevertheless, the structural characterization of such large, morphological features in PBCV-1, CIV, and now PpV01 by means of cryo-EM reconstruction is consistent with the hypothesis that the capsids of these and other similar viruses may involve related assembly intermediates. Assembly may proceed initially via oligomerization of the major capsid protein to form trimeric capsomers, and these capsomers might then aggregate to form trisymmetrons or pentasymmetrons (initiated by interaction with pentameric capsomers comprised of a minor viral protein). The sizes of the trisymmetrons and pentasymmetrons are likely regulated by the presence of minor structural ("cement" or "scaffold") proteins such as those, for example, identified in viruses like adenovirus (14), herpesvirus (29), and PRD1 (1). Regulation of the size of the symmetron would appear to be necessary to ensure accurate assembly of complete capsid shells (from 20 trisymmetrons and 12 pentasymmetrons). Consistent with this notion, there is no evidence of significant polymorphism for any of the large viruses studied thus far.

Numerous other aspects of the assembly of these precise virus capsids remain a mystery. For example, what factor or factors distinguish trimeric capsomers as sites of attachments of fibers? And are capsids assembled around a preassembled, membrane-bound, condensed genome, or instead, is the genome packaged into preformed, empty capsids (6)?

At least one minor protein may be required to solidify the large interfaces ("seams") between the symmetrons. The limited structural data available thus far on large, icosahedral viruses suggest that the size of the pentasymmetron dictates the precise interrelations of neighboring trisymmetrons, whereas the size of the trisymmetron is the principle determinant of the overall size of the capsid. If these assumptions are correct, this could imply that assembly proceeds first via associations between pentasymmetrons and trisymmetrons, followed by interactions between the remaining exposed edges of the trisymmetrons. It may be, as has been elegantly demonstrated in bacteriophage PRD1 (1), that a molecular "tape measure" viral protein is used in PpV01 and other large dsDNA viruses to determine the size of the trisymmetrons and to "cement" them to one another and to the pentasymmetrons.

The most stable "subunit" of the PBCV-1 capsid is the trimer of the 54-kDa major capsid protein (MCP) (25). Based on atomic modeling of the PBCV-1 trimer structure into a 2.8-nm resolution reconstruction of PBCV-1 virions, there appear to be limited or no interactions between the 2,180 trimeric capsomers in the capsid shell (25). This apparent lack of interactions between trimers appears to persist regardless of the different interface that trimers encounter (e.g., within and between tri- and pentasymmetrons). Lack of obvious intertrimeric interactions also appears to be a characteristic of the PpV01 capsid. Hence, intertrimer interactions are not likely to be a primary determinant of capsid stability in large, icosahedral viruses. This is consistent with a belief that there must be a delicate balance between the necessity for capsid stability and a requirement that interactions be weak enough to permit error correction during assembly (30). In adenovirus, for example, polypeptide IX serves as a "cement" protein that tightly couples nine hexons together ("group of nine") at the center of each capsid face and instills stability to the virions (14). Similarly, the minor capsid protein, P30, in bacteriophage PRD1, acts to cement neighboring facets together (1). It seems quite likely that the nearly 15- or 30-fold-larger, by volume, PpV01 (versus adenovirus or PRD1) will incorporate one or more cement proteins (Fig. 3B) to help stabilize its capsid. Additional biochemical characterization and much higher resolution structure analysis of PpV01 are clearly needed to better define the assembly pathway of PpV01 and the existence and role of any putative tape measure or cement proteins.

The large dsDNA icosahedral viruses, such as SIV (33), PBCV-1, CIV (35), FV3 (34), and PpV01 (present study) share a number of common properties that suggest they all evolved from a common ancestor (Table 1) (6): they all include a large dsDNA genome, the MCPs have similar masses and sequences with highly conserved regions (31), they include an internal lipid bilayer, they are encapsidated in a large, well-ordered icosahedral shell primarily composed of trimers of the MCP, and the capsomers are organized in large triangular and pentagonal aggregates (symmetrons). Based on these similarities, it is likely that most if not all other large dsDNA icosahedral

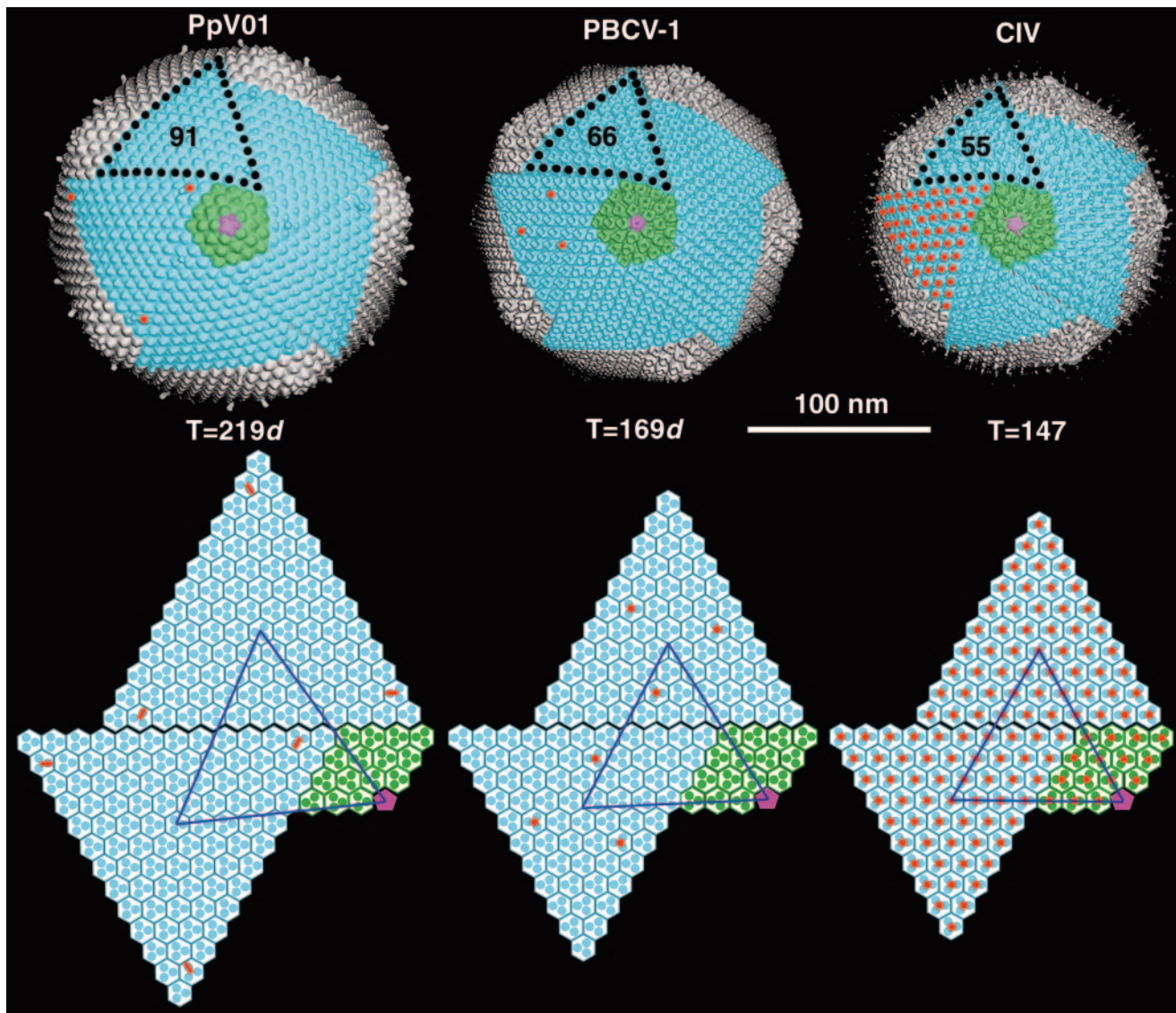


FIG. 4. Trisymmetron and pentasymmetron organization in PpV01, PBCV-1, and CIV. The top row depicts the 3-D reconstructions of three viruses, each with five trisymmetrons colored blue and a single pentasymmetron colored green (trimeric capsomers) and pink (pentamer at vertex). Black circles are used to label the capsomers at the boundary of one trisymmetron in each virus capsid and demonstrate that there are 91, 66, and 55 capsomers in PpV01, PBCV-1, and CIV, respectively. Red circles in one trisymmetron (3 each in PpV01 and PBCV-1 and 55 in CIV) identify the positions of capsomers that contain a fiber (PpV01), a bean-like protrusion (PBCV-1), or a fiber (CIV). In addition, though not labeled in the top row, the 30 trimeric capsomers in the CIV pentasymmetron also contain fibers. Hence in PpV01, PBCV-1, and CIV, there are a total of 60, 60, and 1,460 protrusions, respectively. The bottom row diagrammatically illustrates the organization of trimers (each represented as a hexagon enclosing three circular disks) in the trisymmetrons and pentasymmetrons. For simplicity, the diagram is a planar representation, though the symmetrons are curved structures in native capsids. The open blue triangle outlines one asymmetric unit of the icosahedron. Red bars (PpV01) or disks (PBCV-1 and CIV) depict the positions of the caps, bean-like protrusions, and fibers in these viruses. Pentavalent capsomers are depicted as pink pentagons. All trimers in a given trisymmetron are identically oriented, though the orientation in PBCV-1 is opposite that in CIV and in the dextroenantiomer of PpV01. Each trisymmetron interacts with three trisymmetrons and three pentasymmetrons. The interface between neighboring trisymmetrons appears as a seam, with trimers oppositely oriented in opposing trisymmetrons in all three viruses. In each instance, the seam includes interactions among all but three of the trimers in each trisymmetron edge (10 of 13 in PpV01, 8 of 11 in PBCV-1, and 7 of 10 in CIV). These three trimers contact the trimers in a pentasymmetron. Contrary to the trisymmetrons, the trimers in each pentasymmetron adopt two orientations. This can be seen, for example, by noticing that all but one trimer along the bottom edge of the horizontal seam is identically oriented. Of the six trimers in each asymmetric unit of the pentasymmetron, only four have the same orientation as the trimers in the adjacent trisymmetron (the other two are oppositely oriented).

viruses share these same properties. For example, the significantly larger mimivirus (~400-nm diameter in thin section; 1.2-Mb genome), which was recently discovered in a water tower (23), is very likely related to the other large dsDNA

viruses (6, 26). Like CIV, mimivirus is covered with numerous fibers, and preliminary biochemical analysis has shown that, among 21 proteins identified thus far, 9 are homologous with *Phycodnaviridae* proteins and 5 are homologous with *Iridoviri-*

TABLE 1. Comparative properties of large, spherical dsDNA viruses

Property	Result for:		
	CIV	PBCV-1	PpV01
Family	<i>Iridoviridae</i>	<i>Phycodnaviridae</i>	Unassigned
Diam (nm) ^a	185	190	220
MCP (kDa)	50	54	59
MCP trimer size (nm) ^b	7	7	7
No. of capsomers in trisymmetron	55	66	91
No. of capsomers in pentasymmetron	31	31	31
Total no. of capsomers	1,472	1,692	2,192
T no.	147	169 ^d	219 ^c
No. of fibers/virion	1,460	60	60

^a Maximum diameter measured along 5-fold direction.

^b Diameter.

^c Handedness unknown.

dae proteins (23). The amino acid sequence of the MCP (514 residues) of mimivirus shares 26.8% identity and 37.0% similarity to the Vp54 sequence (6). If mimivirus has an icosahedral capsid organized according to the principles described for viruses like PBCV-1, CIV, SIV, and PpV01, and assuming the number of trimeric capsomers in the icosahedral shell is directly related to shell size, the number of capsomers in mimivirus, and therefore the T number, can be roughly estimated. It is well known that biological specimens tend to shrink when subjected to fixation and dehydration during preparation for thin sectioning and electron microscopy (13). This is certainly true for the large viruses we have studied. The maximum diameters of several large viruses embedded in vitreous ice (34, 35) and their diameters and percent shrinkage when dried in thin section (10, 19, 20) are as follows: PBCV-1, 190 → 160 nm, 16%; CIV, 185 → 145 nm, 22%; FV3, 190 → 145 nm, 24%; PpV01, 220 → 170 nm, 23%. Based on these limited measurements and an estimated shrinkage in the 15 to 25% range, the true diameter of mimivirus is likely to lie somewhere between 470 and 530 Å. Given this range of estimated diameters, the triangulation number for mimivirus could be between 1,078 and 1,371, which would correspond to a total number of capsomers [=10 × (T - 1) + 12] ranging between 10,782 and 13,712. There are 183 different combinations of *h* and *k* that describe the potential lattice symmetries represented in this range of T numbers. Regardless of what lattice symmetry the mimivirus capsid actually possesses, it is predicted to have a much larger T number and number of capsomers than PpV01.

ACKNOWLEDGMENTS

We thank J. Van Etten for initiating this study and V. Bowman for collecting preliminary cryo-EM images of PpV01 at 200 keV in an FEI/Philips CM200 microscope. We also thank C. Xiao and R. Ashmore for assistance with programming and J. Van Etten, W. Zhang, and X. Zhang for helpful discussions and suggestions.

The research was supported in part by grants from the NIH (GM-33050 and AI-45976) and NSF (MCB-9206305) to T.S.B., by a grant from The Research Council of Norway (project no. 121425/420) to G. Bratbak, and by an award to the Purdue Structural Biology Group from the Keck Foundation for the purchase of the CM300 FEG microscope.

REFERENCES

- Abrescia, N. G., J. J. Cockburn, J. M. Grimes, G. C. Sutton, J. M. Diprose, S. J. Butcher, S. D. Fuller, C. San Martin, R. M. Burnett, D. I. Stuart, D. H. Bamford, and J. K. Bamford. 2004. Insights into assembly from structural analysis of bacteriophage PRD1. *Nature* **432**:68–74.
- Baker, T. S., and R. H. Cheng. 1996. A model-based approach for determining orientations of biological macromolecules imaged by cryoelectron microscopy. *J. Struct. Biol.* **116**:120–130.
- Baker, T. S., N. H. Olson, and S. D. Fuller. 1999. Adding the third dimension to virus life cycles: three-dimensional reconstruction of icosahedral viruses from cryo-electron micrographs. *Microbiol. Mol. Biol. Rev.* **63**:862–922.
- Bates, T. S., B. K. Lamb, A. Guenther, J. Dignon, and R. E. Stoiber. 1992. Sulfur emission to the atmosphere from natural sources. *J. Atmos. Chem.* **14**:315–337.
- Belnap, D. M., N. H. Olson, and T. S. Baker. 1997. A method for establishing the handedness of biological macromolecules. *J. Struct. Biol.* **120**:44–51.
- Benson, S. D., J. K. Bamford, D. H. Bamford, and R. M. Burnett. 2004. Does common architecture reveal a viral lineage spanning all three domains of life? *Mol. Cell* **16**:673–685.
- Brussard, C. P. D., R. Riegman, A. A. Noordeloos, G. C. Cadée, H. Witte, A. J. Kop, G. Nieuwland, F. C. van Duyl, and R. P. M. Bak. 1995. Effects of grazing, sedimentation and phytoplankton cell lysis on the structure of a coastal pelagic food web. *Mar. Ecol. Prog. Ser.* **123**:259–271.
- Caspar, D. L., and A. Klug. 1962. Physical principles in the construction of regular viruses. *Cold Spring Harb. Symp. Quant. Biol.* **27**:1–24.
- Castberg, T., R. Thyraug, A. Larsen, R.-A. Sandaa, M. Hedal, J. L. Van Etten, and G. Bratbak. 2002. Isolation and characterization of a virus that infects *Emiliania huxleyi* (Haptophyceae). *J. Phycol.* **38**:767–774.
- Cuillé, M., F. Tripiet, J. Braunwald, and B. Jacrot. 1979. A low resolution structure of frog virus 3. *Virology* **99**:277–285.
- Davidson, A. T., and H. J. Marchant. 1992. The biology and ecology of Phaeocystis (Prymnesiophyceae). *Prog. Phycol. Res.* **8**:1–45.
- DeRosier, D. J. 2000. Correction of high-resolution data for curvature of the Ewald sphere. *Ultramicroscopy* **81**:83–98.
- Earnshaw, W. C., J. King, and F. A. Eiserling. 1978. The size of the bacteriophage T4 head in solution with comments about the dimension of virus particles as visualized by electron microscopy. *J. Mol. Biol.* **122**:247–253.
- Furcinitti, P. S., J. van Oostrum, and R. M. Burnett. 1989. Adenovirus polypeptide IX revealed as capsid cement by difference images from electron microscopy and crystallography. *EMBO J.* **8**:3563–3570.
- Guillard, R. R. L. 1975. Culture of phytoplankton for feeding marine invertebrates, p. 26–60. *In* W. L. Smith and M. H. Chanley (ed.), *Culture of marine invertebrate animals*. Plenum Press, New York, N.Y.
- Iyer, L. M., L. Aravind, and E. V. Koonin. 2001. Common origin of four diverse families of large eukaryotic DNA viruses. *J. Virol.* **75**:11720–11734.
- Jacobsen, A., G. Bratbak, and M. Heldal. 1996. Isolation and characterisation of a virus infecting *Phaeocystis pouchetii* (Prymnesiophyceae). *J. Phycol.* **32**:923–927.
- Jensen, G. J., and R. D. Kornberg. 2000. Defocus-gradient corrected back-projection. *Ultramicroscopy* **84**:57–64.
- Kawakami, H., and N. Kawakami. 1978. Behavior of a virus in a symbiotic system, *Paramecium bursaria-zoochlorella*. *J. Protozool.* **25**:217–225.
- Kelly, D. C., and T. W. Tinsley. 1974. Iridescent virus replication: a microscope study of *Aedes aegypti* and *Anthera eucalypti* cells in culture infected with iridescent virus types 2 and 6. *Microbios* **9**:75–93.
- Lancelot, C., G. Billen, A. Sournia, T. Weisse, F. Coljin, M. Veldhuis, A. Davies, and P. Wassman. 1987. Phaeocystis blooms and nutrient enrichment in the continental coastal zones of the North Sea. *Ambio* **16**:38–46.
- Lancelot, C., P. Wassmann, and H. Barth. 1994. Ecology of Phaeocystis-dominated ecosystems. *J. Mar. Syst.* **5**:1–4.
- La Scola, B., S. Audic, C. Robert, L. Jungang, X. de Lamballerie, M. Drancourt, R. Birtles, J. M. Claverie, and D. Raoult. 2003. A giant virus in amoebae. *Science* **299**:2033.
- Malin, G., W. H. Wilson, G. Bratbak, P. S. Liss, and N. H. Mann. 1998. Elevated production of dimethylsulfide resulting from viral infection of cultures of *Phaeocystis pouchetii*. *Limnol. Oceanogr.* **43**:1389–1393.
- Nandhagopal, N., A. A. Simpson, J. R. Gurnon, X. Yan, T. S. Baker, M. V. Graves, J. L. Van Etten, and M. G. Rossmann. 2002. The structure and evolution of the major capsid protein of a large, lipid-containing DNA virus. *Proc. Natl. Acad. Sci. USA* **99**:14758–14763.
- Raoult, D., S. Audic, C. Robert, C. Abergel, P. Renesto, H. Ogata, B. La Scola, M. Suzan, and J. M. Claverie. 2004. The 1.2-megabase genome sequence of Mimivirus. *Science* **306**:1344–1350.
- Rayment, I., T. S. Baker, D. L. Caspar, and W. T. Murakami. 1982. Polyoma virus capsid structure at 22.5 Å resolution. *Nature* **295**:110–115.
- Rux, J. J., P. R. Kuser, and R. M. Burnett. 2003. Structural and phylogenetic analysis of adenovirus hexons by use of high-resolution X-ray crystallographic, molecular modeling, and sequence-based methods. *J. Virol.* **77**:9553–9566.
- Spencer, J. V., W. W. Newcomb, D. R. Thomsen, F. L. Homa, and J. C.

- Brown.** 1998. Assembly of the herpes simplex virus capsid: preformed triplexes bind to the nascent capsid. *J. Virol.* **72**:3944–3951.
30. **Stewart, P. L., R. M. Burnett, M. Cyrklaff, and S. D. Fuller.** 1991. Image reconstruction reveals the complex molecular organization of adenovirus. *Cell* **67**:145–154.
31. **Tidona, C. A., P. Schnitzler, R. Kehm, and G. Darai.** 1998. Is the major capsid protein of iridoviruses a suitable target for the study of viral evolution? *Virus Genes* **16**:59–66.
32. **Van Etten, J. L.** 2003. Unusual life style of giant chlorella viruses. *Annu. Rev. Genet.* **37**:153–195.
33. **Wrigley, N. G.** 1969. An electron microscope study of the structure of Sericesthis iridescent virus. *J. Gen. Virol.* **5**:123–134.
34. **Yan, X., V. Bowman, G. Murti, R. Goorha, A. Hyatt, and T. S. Baker.** 2001. 3D image reconstruction of frog virus 3 at 2.6 nm. *Microsc. Microanal.* **7**:746–747.
35. **Yan, X., N. H. Olson, J. L. Van Etten, M. Bergoin, M. G. Rossmann, and T. S. Baker.** 2000. Structure and assembly of large lipid-containing dsDNA viruses. *Nat. Struct. Biol.* **7**:101–103.
36. **Zhang, X., S. Walker, P. R. Chipman, M. L. Nibert, and T. S. Baker.** 2003. Reovirus polymerase $\lambda 3$ localized by cryo-electron microscopy of virions at a resolution of 7.6 Å. *Nat. Struct. Biol.* **10**:1011–1018.
37. **Zhao, R., D. C. Pevear, M. J. Kremer, V. L. Giranda, J. A. Kofron, R. J. Kuhn, and M. G. Rossmann.** 1996. Human rhinovirus 3 at 3.0 Å resolution. *Structure* **4**:1205–1220.